Mechanical resonance properties of porous graphene membrane; simulation study and proof of concept experiment

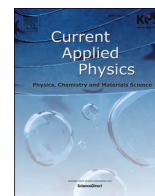Yoon, Juhee; Kwon, Min Hee; Shin, Dong Hoon; Lee, Sang Wook

Important note
To cite this publication, please use the final published version (if applicable).
Please check the document version above.

Mechanical resonance properties of porous graphene membrane; simulation study and proof of concept experiment

Juhee Yoon [a], Min Hee Kwon [a,1], Dong Hoon Shin [a,b,**], Sang Wook Lee [a,*]

[a] *Department of Physics, Ewha Womans University, Seoul, 03760, South Korea*
[b] *Kavli Institute of Nanoscience, Delft University of Technology, Lorentzweg 1, 2628 CJ, Delft, The Netherlands*

A B S T R A C T

Mechanical resonance properties of porous graphene resonators were investigated by simulation studies. The finite element method was utilized to design the porous graphene membrane pattern and to calculate the mechanical resonance frequency and quality factor. The changes in the resonance frequency and quality factor were systematically studied by changing the size, number, and relative location of pores on the graphene membrane. Mass loss and carbon-carbon bond break were found to be the main competing parameters for determining its mechanical resonance properties. The correlation between the geometry and the damping effect on the mechanical resonance of graphene was considered by suggesting a model on the damping factor and by calculating the membrane deflections according to the pore location. Based on the simulation results, an optimal porosity and porous geometry were found that gives the maximum resonance frequency and quality factor. Suspended graphene with various number pore structures was experimentally realized, and their mechanical resonance behaviors were measured. The trend of changes in resonance frequency and quality factor according to the number of pores in the experiment was qualitatively agreed with simulation results.

1. Introduction

Since graphene was exfoliated from graphite flakes [1], an enormous amount of studies have been reported on the physical properties and applications [2–4]. Its two-dimensional nature offers a lot of interesting quantum mechanical phenomena, such as the quantum Hall effect [5], valley states [6], quantum electron optics [7], and so on. Graphene receives anew spotlights as it recently showed superconductivity and Mott insulator states [8], which are unexpected and emerging phenomena, from bilayer graphene with a specific twisted angle. Besides the aforementioned phenomena, which mainly originate from electrical properties, graphene also has superior mechanical properties with high strength, high flexibility, and light mass [9]. However, the research on graphene-based mechanical or electromechanical systems has been relatively less investigated than electrical studies.

Nanoelectromechanical systems (NEMS) combine mechanical and electrical degrees of freedom with nanoscale, which enables higher sensitivity than other electrical devices as they utilize two orthogonal information, that is, mechanical and electrical information [10].

Graphene can be one of the best candidate materials for NEMS since it has good electrical conductivity as well as high mechanical strength [11]. Recent reports showed that it was possible to achieve a 'quantum mechanical' phenomena [12] and an ultra-sensitive mechanical measurement [13] using graphene-based nanoelectromechanical devices. To improve the device performance of graphene NEMS, it is necessary to increase the mechanical resonance frequency and quality (Q) factor. However, it was found from the previously reported works that the resonance frequency and Q factor of graphene nanomechanical resonator, realized in experiments, were much less than theoretically estimated values [14].

We have especially focused on the effect of damping on the graphene resonator, which is a crucial factor in degrading the mechanical performances of devices. In the case of the microelectromechanical system (MEMS), there have been many trials to solve this issue. One of the most suitable methods is defining a porous structure on the MEMS resonator [15–17]. The hole patterns on the resonator material help the Q factor increase by reducing the damping parameter, and the resonance frequency increases by reducing the effective mass. In this work, we
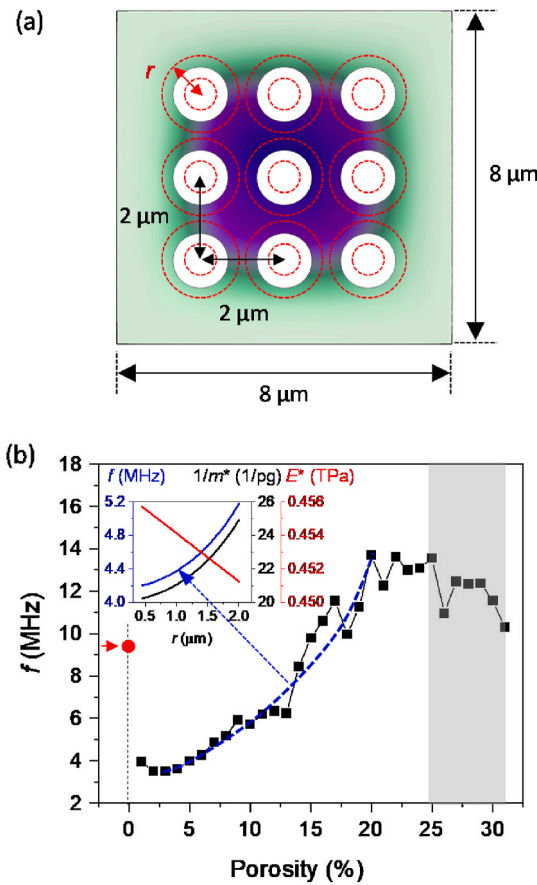
(a)

(b)

Fig. 1. (a) The Geometry and the mechanical resonance mode of a suspended graphene membrane. The area of the suspended membrane is 8×8 μm^2, and the distance between the centers of each pore is 2 μm. (b) Porosity dependent mechanical resonance frequency. The inset graph in (b) shows the porosity dependent resonance frequency, effective mass, and Young's modulus changes calculated by the suggested model.

adapted the above-mentioned idea of MEMS to the graphene nano-mechanical resonator. Graphene resonators with various porous patterns were designed, and their mechanical resonance properties were studied by the finite element method. Based on the modeling and simulation work, the optimal geometry of the graphene resonator could be suggested. The graphene resonator with hole structures was realized by nanofabrication. The measured mechanical properties of graphene resonators in experiments were qualitatively consistent with the simulation results.

2. Simulation method and result

COMSOL Multiphysics with finite element analysis is used for simulating porous graphene geometry. This method assumes that the structure under test consists of small pieces, and the equations of motion on each piece are integrated and formulates into one equation. Then, a numerical analysis of the equation is conducted for determining the significant features of mechanical behavior on the entire structure. To study the resonance behaviors of porous graphene resonators, we used the structural mechanics module of COMSOL Multiphysics, which is customized to analyze the mechanical properties of structures, such as stress, strain, stiffness, flexibility, and the mechanical resonance frequency. The radius, position, and the number of pores at the membrane were varied as the control parameters in this simulation while the size of the graphene membrane was set to 8 μm × 8 μm. These parameters affect the spring constant and mass of the membrane, and, consequently, the resonance frequency and Q factor of graphene resonator were changed.

Firstly, we calculated the porosity-dependent mechanical resonance frequency of the graphene membrane. For an initial condition to study the effect of porosity, we selected a 3×3 array of pores and kept the distance between the centers of each pore to be 2 μm as shown in Fig. 1 (a). Then we changed the radius of the pores to modulate the porosity of the membrane. Fig. 1(b) shows the simulation result of the resonance frequency changes as the porosity varies from 1% to 31%. The red dot indicates the resonance frequency of the graphene membrane with no pore. Once a pore structure with 1% of porosity is defined, the resonance frequency suddenly dropped to around 45% of the initial value, which implies that a few defects on the graphene surface could give a significant reduction of its mechanical strength. It is considered for understanding this result on porosity-dependent resonance frequency that there are two main competing aspects to determine the resonance frequency of the porous membrane. First, the number of defects, which arises from the broken carbon bonding increases when the size of the pore becomes larger. Therefore, the stiffness caused by Young's modulus (E) of the graphene membrane is weakened so that the resonance frequency could be reduced. Second, the void of carbon atom increases when the size of the pore becomes larger. As a consequence, the effective mass (m) of the resonator decreases so that the resonance frequency could be enhanced.

The relationship between mass density and the Young's modulus to the mechanical resonance frequency of a membrane can be presented as the following equation [14],

$$f_0 = \alpha \sqrt{\frac{E}{\rho}} \frac{t}{L^2}$$

where t and L are thickness and suspended length of the graphene membrane, α is the clamping coefficient, E is Young's modulus, ρ is the mass density. Since we defined the circular pores on the graphene membrane, the size of the void area, which is directly related to the loss of effective mass, is proportional to the square of the radius of each pore.

On the other hand, the broken carbon bonding by void area reduces the spring constant of the membrane. The broken carbon bonding appears at the circumference of pores. Consequently, the Young's modulus of the graphene membrane, which is proportional to the spring constant, is decreased by increasing the circumference of the pore as the void area enlarged [18–20].

According to the above-mentioned condition, the effective mass and Young's modulus of a graphene membrane can be presented with a radius (r) as follows.

$$m^* = m_0 \left(1 - \frac{\pi r^2}{A} \right)$$

$$E^* = E_0 (1 - \beta 2 \pi r)$$

where A is 64 μm^2 in our model, β is a proportional constant for decreasing Young's modulus.

The inset of Fig. 1(b) plots the resonance frequency changes depending on the radius of the pore on the membrane. It reveals that the effect of mass reduction is more dominant than that of stiffness weakening as the radius of the circular hole increases. The two-dimensional geometry of graphene could give a more dramatic effect of mass reduction to the resonator compared to MEMS resonators that have bulky three-dimensional structures.

Overall, the simulation results on the porosity dependence of resonance frequency can be understood as follows. Upon the porous defects being created on the graphene, a significant amount of resonance frequency value of the membrane is dropped down. The reduction rate of the mass is more sensitively affected than that of stiffness to the graphene membrane so that the resonance frequency is gradually increased until 25% of porosity. From the porosity range higher than 25% (a shaded area in Fig. 1(b)), the frequency is found to drop again, which is
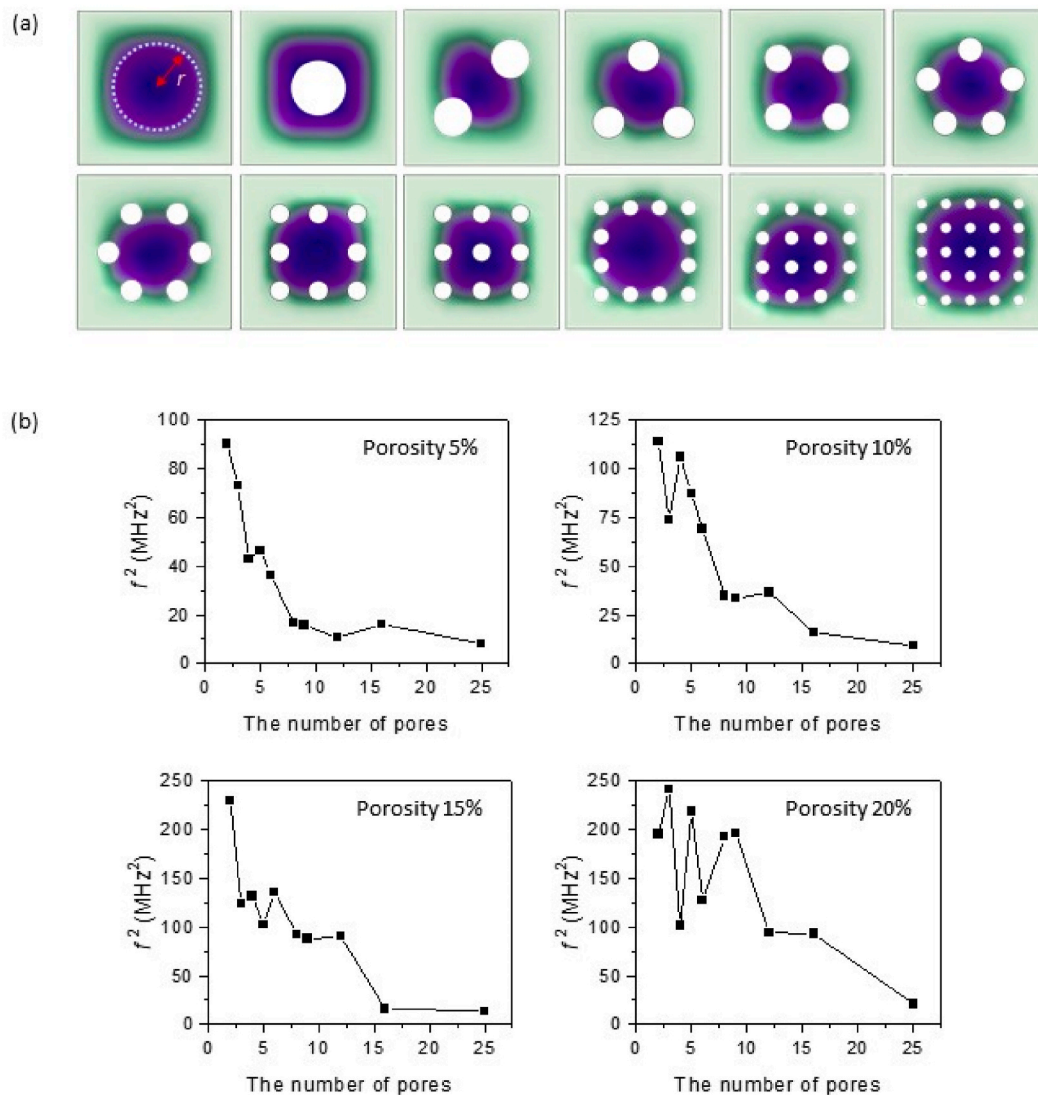
Fig. 2. (a) Geometric models and mechanical resonance modes of porous graphene membrane. (b) Resonance frequency of membrane according to the number of pores at a given porosity.

considered due to the failure of stiffness maintenance by too many defects on the membrane. This reflects that there is a certain limit of porosity to increase the resonance frequency of the graphene resonator.

More systematic simulation work was performed to determine the Young's moduli of the membrane with different geometries. Fig. 2 is the simulation result of resonance frequency on graphene membranes according to the number of pores while keeping the porosity constant. Fig. 2(a) shows the geometry of the membrane defined for this simulation study. The number of arrays was increased by keeping the distance between the pores constant. In the case of 2, 3, 5, and 6 pores, which cannot be defined by a specific design rule, the pores were positioned with a distance of 2 μm apart from the center of the membrane. 8 and 12 pores, in particular, the pore(s) positioned at the center of the membrane was (were) omitted for convenience of simulation.

Fig. 2(b) shows the calculated mechanical resonance frequency with the porosity of 5, 10, 15, and 20%, respectively. The resonance frequency decreases as the number of pores increases for all porosity cases. Since the porosity of the membrane was kept constant for each simulation, the resonance frequency lowering as an increasing number of pores originated not from the mass change but from the suppression of Young's modulus. The sum of the circumference of pores with radius r is calculated to be $2\pi nr$ according to the number (n) of pores. Since the

amount of broken carbon bonding is proportional to the circumference of pores as it was modeled in the previous section, the Young's modulus of membrane reduced with increasing pore numbers. Although the overall tendency of frequency decrease follows the number of broken carbon bonding, there are some noticeable fluctuations on the pore number dependent resonance frequency curves at the simulation result. This implies that the resonance frequency of our membrane structure can be affected by the geometry of pores as well.

To verify the effect of the geometrical factor of pores on the mechanical properties of the membrane, we investigated the change in the resonance frequency by rotating the array of pores as shown in Fig. 3. A hexagonal array of pores was defined on the membrane, and the resonance frequency was calculated by rotating the array with 45 and 90° in counter-clockwise. The simulation result under this condition shows that, in the case of a square membrane as shown in Fig. 3(a), the resonance frequency fluctuates up to 15% higher than the initial position of pores by merely rotating the pore array pattern as indicated by black squares in Fig. 3(c). As the pore array pattern rotates, the distance between the edge of the membrane and each pore changes. Accordingly, changes in the mass distribution due to repositioning of the pores appear to be sensitive to the resonant behavior of the rectangular membrane. To complement our deduction, we simulated the resonance frequency of a
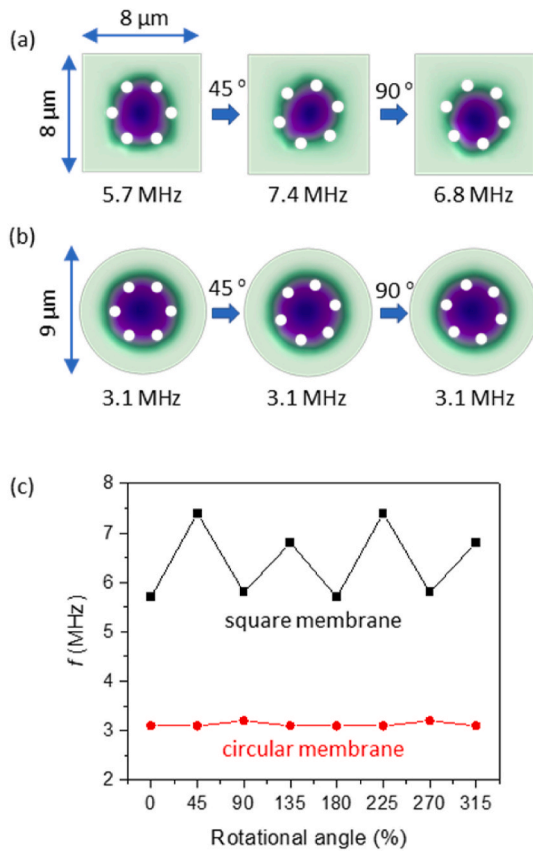
Fig. 3. The geometry of square membrane (a), and circular membrane (b) for studying rotation dependent mechanical resonance frequency variation. The resonance frequency changes only in the square membrane. (c) Simulation results on the variation of mechanical resonance frequency by rotating position of pores for both cases.

Fig. 4. Cross-sectional (a) and top (b) view of graphene membrane in the 1st resonance mode with 5% of porosity. z is the vibrational displacement of the membrane, and l is the cross-sectional length of the square membrane. The length of the straight line from the center of the membrane to the edge of the pore is r, and the length from the center of the pore to the edge of the membrane is d. (c) Deflection ratio between nonporous (Z_0) and porous (Z) membrane depending on the position of a single pore.

circular membrane with the same hexagon array of pores as shown in Fig. 3(b). Since the distance between the pore and circular membrane edge is constant in all rotational angles, no frequency change appeared at this configuration as indicated by red dots in Fig. 3(c). To summarize the simulation results, the mass and stiffness changes due to the porosity and the number of pores are the main competing parameters to determine the resonance frequency of the graphene membrane. In addition to this, the variation of the geometric structure of pores can give a meaningful fluctuation to the resonance frequency.

Secondly, we investigated the dependence of the Q factor on the geometry of pores. Since a capacitive force (F_c) is applied to drive the mechanical resonance of graphene in our experimental system and phenomenological damping ($\gamma_d \dot{x}$) can be introduced to our system, the equation of motion for our graphene membrane with effective mass m_{eff} and spring constant k can be introduced as follows:

$$m_{eff}\ddot{x} = -kx - \gamma_d\dot{x} + F_c$$

$$\left(-\omega^2 m + (1+i\gamma)k\right)\tilde{x} = \tilde{F}$$

The damping will be relieved where the pores exist on the membrane so that the dissipation of resonance can be reduced by increasing the porosity of the membrane. It should also be noted that the amount of damping is strongly affected by the geometry of pores since the vibrational velocity of the resonator depends on the position on the graphene membrane. Fig. 4 (a) shows the cross-section view of displacement of the graphene membrane on resonance. The amplitude and vibrational velocity of the membrane becomes maximum (or minimum) at the center (or edge) of the suspended membrane. Thus, the closer the pores were placed to the center of suspended graphene, the more damping effect
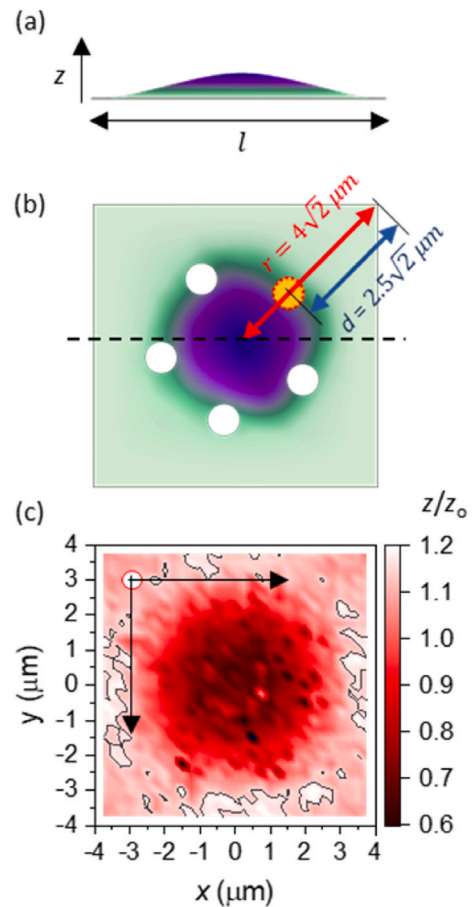
can be compensated. Since the vibrational amplitude is much smaller than the suspended length of the membrane ($z \ll l$ in Fig. 4(a)), we assume that the vibrational amplitude velocity has linear variation along the suspended graphene. By considering the damping of the membrane according to the position of each pore, the geometry dependent damping effect on the porous graphene structure can be applied to our simulation. According to the above-mentioned description, the position-dependent damping parameter at given porosity P can be expressed as

$$P \times \frac{1}{N}\sum_{n=1}^{N}\frac{d_n}{r_n}$$

where N is the total number of pores, r is suspended length from center to the edge crossing pore, d is the distance from the pore to the edge of the suspended membrane indicated in Fig. 4(b).

For example, if we consider a porous membrane as shown in Fig. 4 (b), the amount of damping at the dashed circle can be expressed as $P \times \frac{1}{5} \times 5 \times \frac{2.5}{4}$. When this dashed area becomes a pore, the calculated amount of damping will be relieved, which affects the initial damping loss factor (γ_i). Therefore, the mechanical resonance behavior of porous graphene can be simulated by considering the finally derived damping loss factor (γ_f), which is formulated as follows:

$$\gamma_f = \gamma_i\left(1 - P\frac{1}{N}\sum_{n=1}^{N}\frac{d_n}{r_n}\right)$$

Table 1

Simulation results on the resonance frequency and *Q* factor of graphene membrane by generating pore structures with various geometry, porosity, and number of pores.

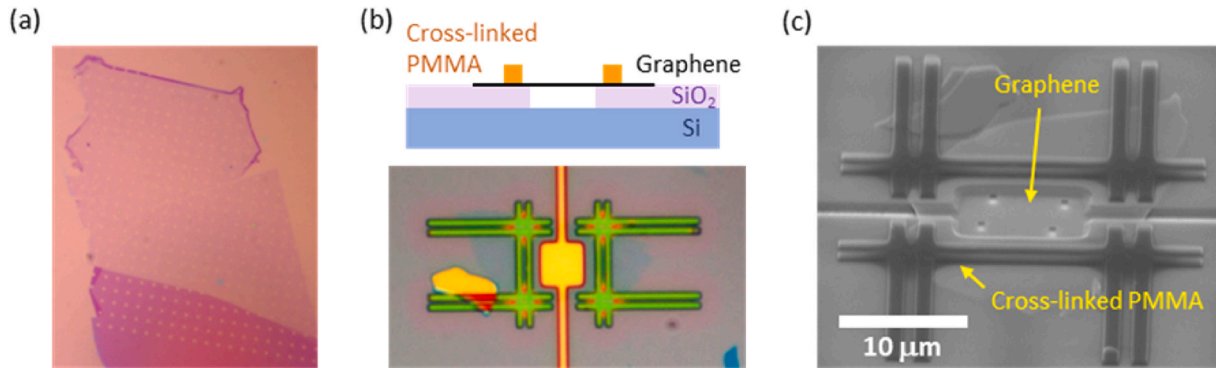| Geometry										
Porosity [%]	0	5	10	10	10	15	15	20	20	20
No. of pores	0	5	4	5	12	4	6	3	5	6
f [MHz]	9.41	8.29	9.82	9.49	7.86	14.6	14.86	16.11	15.36	12.93
Q factor	181.82	187.54	193.94	193.57	192.27	200.65	196.55	211.39	207.77	202.02

Fig. 5. (a) The optical microscope image of exfoliated monolayer graphene with pores. (b) A schematic of a suspended graphene resonator device (top) and the optical microscope image of suspended graphene transferred on the trench substrate. (c) Scanning electron microscope image of graphene resonator device with 2 × 2 pore structures. The scale bar shows 10 μm.

While varying the porosity from 5% to 20%, we calculate the *Q* factor and resonance frequency of graphene resonators according to the geometry of pores on the membrane. The initial damping coefficient γ_i was set to 0.6 so that around 182 of the *Q* factor of a graphene resonator without pore structure can be obtained by simulation. This value is matched to our previously reported experimental measurements on the resonance frequency of graphene resonator with a low vacuum condition ($\sim 10^{-4}$ torr) [18,19].

For finding the optimal geometry of pores, which gives a high *Q* factor value, a deflection of graphene membrane in *z*-direction according to the pore position was studied. The position of a pore, as indicated with a red circle in Fig. 4(c), with 500 nm diameter is placed on the membrane and the vibrational displacement in *z*-direction was calculated. Fig. 4(c) shows the mapping result on the ratio of the average value of membrane deflection between nonporous (Z_0) and porous (Z) as scanning the position of a pore. It was found that the deflection of the membrane was more suppressed when a pore was created at the center of the membrane. Since the deflection of the membrane is related to the damping factor, this result means that more *Q* factor increase can be expected by placing the pores on the central area of the membrane, which is consistent with our suggested modeling. On the other hand, the average deflection value was even increased when the pores were created on the edge of the membrane. This result suggested that there is an optimal positioning of the arrangement of pores of which gives lower damping factors. Also, the deflection mapping result tells that the circular arrangement of pores looks more efficient to increase the *Q* factor of the graphene membrane.

Table 1 shows the simulation results of the mechanical resonance frequency and *Q* factor of the graphene membrane with various porous geometries after applying the damping loss factor at each pore position. The highest *Q* factor value was found at 20% of porosity with three circular pores surrounding the center of the membrane. The maximum value of resonance frequency also appears at 20% of porosity.
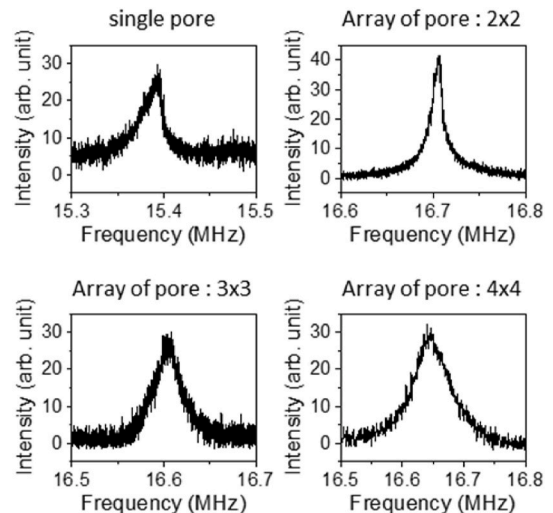

Fig. 6. Measurement results of the mechanical resonance frequencies of four graphene resonator devices with a various number of pores.

3. Experimental

The mechanical properties of suspended graphene resonator devices were investigated to compare the simulation results. Graphene flakes for the resonator device were produced by a mechanical exfoliation method. The nanoscale pore structures were defined on top of the pre-deposited graphene flakes using electron beam lithography followed by oxygen plasma etching. Fig. 5(a) shows an optical microscope image of an exfoliated graphene with porous hole patterns. The graphene flake with pore structure was transferred to the target substrate, where a trench and a bottom electrode were fabricated. PMMA was used as a transfer media on this process. After positioning the graphene flake, an excessive dose of the electron beam ($\sim$15,000 μC/cm^2) was exposed to

the PMMA layer around the trench structure, forming a locally cross-linked PMMA to clamp the ends of the graphene. Fig. 5(b) and (c) show the schematics and optical image of the device structure and scanning electron microscope image of a graphene resonator device, respectively. The diameter of each hole is kept to be 500 nm, and the number of pores on the suspended graphene area was varied by 1, 4 (2 × 2), 9 (3 × 3), and 16 (4 × 4). The resonance behavior of the suspended porous graphene structure was measured by the laser interferometry method [20,21].

Fig. 6 shows the measurement results of the mechanical resonance of 4 graphene devices, which were successfully fabricated, with a various number of pores. Both the resonance frequency and the Q factor value increase and show the maximum value on the membrane with 2 × 2 pore structures, then the frequency decreases. The practically measured frequency and estimated Q factor values did not perfectly follow the ideal numbers from the simulation works since there should be unavoidable error sources on the graphene devices such as defects on graphene, residues on the surface, ripples in the suspended membrane, initial tension on the devices and so on. However, even though a small number of devices with several error factors, the experimental results of the graphene resonator are qualitatively consistent with simulation work.

4. Summary

In summary, the mechanical resonance properties of the porous graphene membrane were studied by the finite element method, and the simulated results were compared with experimental test devices. The mechanical resonance frequency of the membrane was calculated by varying the porosity of the graphene membrane, the number of pores, and the geometry of pore patterns. Mass loss and carbon-carbon bond break are two main competing parameters for determining resonance frequency values. The Q factor of suspended graphene membrane depends on the position and geometry of the pore structures as well as porosity. It was found that mechanical resonance properties of the two-dimensional graphene membrane were more sensitively modified by creating pore structures compare to three-dimensional MEMS structures. Based on the simulation results, a geometry of surrounded circular pores with 20% of porosity provides the maximum resonance frequency and Q factor to the suspended graphene membrane. Based on the modeling, suspended graphene with a various number of pore structures was realized in the experiment, and their mechanical resonance behaviors were measured. The tendency of frequency and Q factor variation according to the pore numbers in the experiment qualitatively agrees with simulation results.

Declaration of competing interest

The authors declare that they have no known competing financial interests or personal relationships that could have appeared to influence the work reported in this paper.

References

[1] K.S. Novoselov, et al., Electric field effect in atomically thin carbon films, Science 306 (5696) (2004) 666–669.

[2] K.S. Kim, et al., Large-scale pattern growth of graphene films for stretchable transparent electrodes, Nature 457 (7230) (2009) 706–710.

[3] P.R. Wallace, The band theory of graphite, Phys. Rev. 71 (9) (1947) 622–634.

[4] C. Lee, et al., Measurement of the elastic properties and intrinsic strength of monolayer graphene, Science 321 (5887) (2008) 385–388.

[5] Y. Zhang, et al., Experimental observation of the quantum Hall effect and Berry's phase in graphene, Nature 438 (7065) (2005) 201–204.

[6] E. McCann, et al., Weak-localization magnetoresistance and valley symmetry in graphene, Phys. Rev. Lett. 97 (14) (2006) 146805.

[7] V.V. Cheianov, V. Fal'ko, B. Altshuler, The focusing of electron flow and a Veselago lens in graphene pn junctions, Science 315 (5816) (2007) 1252–1255.

[8] Y. Cao, et al., Unconventional superconductivity in magic-angle graphene superlattices, Nature 556 (7699) (2018) 43–50.

[9] I. Frank, et al., Mechanical properties of suspended graphene sheets, J. Vac. Sci. Technol. B: Microelectron.Nanometer. Struct.Process . Meas. Phenom. 25 (6) (2007) 2558–2561.

[10] K.L. Ekinci, M.L. Roukes, Nanoelectromechanical systems, Rev. Sci. Instrum. 76 (6) (2005).

[11] M. Poot, H.S. van der Zant, Nanomechanical properties of few-layer graphene membranes, Appl. Phys. Lett. 92 (6) (2008), 063111.

[12] V. Singh, et al., Optomechanical coupling between a multilayer graphene mechanical resonator and a superconducting microwave cavity, Nat. Nanotechnol. 9 (10) (2014) 820–824.

[13] G. Luo, et al., Coupling graphene nanomechanical motion to a single-electron transistor, Nanoscale 9 (17) (2017) 5608–5614.

[14] J.S. Bunch, et al., Electromechanical resonators from graphene sheets, Science 315 (5811) (2007) 490–493.

[15] W. Benecke, A. Splinter, MEMS applications of porous silicon, in: Device and Process Technologies for MEMS and Microelectronics II, International Society for Optics and Photonics, 2001.

[16] A. Kovacs, et al., Mechanical investigation of perforated and porous membranes for micro-and nanofilter applications, Sensor. Actuator. B Chem. 127 (1) (2007) 120–125.

[17] C. Tu, J.-Y. Lee, Enhancing quality factor by etch holes in piezoelectric-on-silicon lateral mode resonators, Sensor Actuator Phys. 259 (2017) 144–151.

[18] M.F. El-Kady, et al., Laser scribing of high-performance and flexible graphene-based electrochemical capacitors, Science 335 (6074) (2012) 1326–1330.

[19] D.H. Shin, H. Kim, S.W. Lee, Nanoelectromechanical graphene switches for the multi-valued logic systems, Nanotechnology 30 (36) (2019) 364005.

[20] T. Kouh, et al., Diffraction effects in optical interferometric displacement detection in nanoelectromechanical systems, Appl. Phys. Lett. 86 (1) (2005), 013106.

[21] D.W. Carr, et al., Measurement of mechanical resonance and losses in nanometer scale silicon wires, Appl. Phys. Lett. 75 (7) (1999) 920–922.